Journal of Solid State Chemistry **154,** 361–367 (2000)
doi:10.1006/jssc.2000.8796, available online at http://www.idealibrary.com on IDEAL®

Neutron Diffraction Study of the Structural Distortions in $Sr_3Ru_2O_7$

H. Shaked[1] and J. D. Jorgensen

Materials Science Division, Argonne National Laboratory, Argonne, Illinois 60439

O. Chmaissem

Physics Department, Northern Illinois University, Dekalb Illinois 60115; and Materials Science Division, Argonne National Laboratory, Argonne, Illinois 60439

S. Ikeda[2]

Department of Physics, Kyoto University, Kyoto 606-8502, Japan

and

Y. Maeno

Department of Physics, Kyoto University, Kyoto 606-8502, Japan; and Core Research for Evolutionary Science, Japan Science and Technology Corporation, Kawaguchi, Saitama 332-0012, Japan

Received March 14, 2000; in revised form May 31, 2000; accepted June 16, 2000; published online August 30, 2000

It is shown that due to the ionic sizes of Sr^{2+} and Ru^{4+}, crystal structure distortions are expected in the layered structure of $Sr_3Ru_2O_7$. Using neutron powder diffraction of $Sr_3Ru_2O_7$, the expected distortions are indeed found and their nature is studied at room temperature. It is found that among the eight possible modes of pure rotations (i.e., rotations along symmetry axes) of the oxygen octahedra, only one mode is consistent with the neutron data. In this mode the octahedra rotate about the *c* axis with intra- and interbilayer order. This ordered model is in contrast to a previously reported semi-ordered model, where the rotations in every other bilayer have interbilayer disorder.

Key Words: **bilayered perovskites; structural distortions; $Sr_3Ru_2O_7$; neutron diffraction.**

INTRODUCTION

The discovery of high-temperature superconductivity in layered perovskites (1), low-temperature superconductivity in Sr_2RuO_4 (2), which has single layers of RuO_6 octahedra, and the remarkable magnetoresistive properties in layered manganese oxides (3) renewed interest in the structural and physical properties of the corresponding two-layer compound $Sr_3Ru_2O_7$ (4–6). In two studies it was found that $Sr_3Ru_2O_7$ is paramagnetic above ~ 150 K ($\mu_{eff} \sim 2.8\ \mu_B$) and shows a magnetic transition at ~ 20 K (4, 5). These results cast doubt (5) on a study by Cao *et al.* (6), who had reported that $Sr_3Ru_2O_7$ exhibits ferromagnetism below 104 K with an additional transformation occurring at 66 K. The electrical resistivity of $Sr_3Ru_2O_7$ is metal-like, with $\rho_{ab} \ll \rho_c$, showing a sharp change in the slope of ρ_c at ~ 50 K, and of ρ_{ab} at ~ 20 K (5, 6). Determination of the precise nature of the structural distortions (see below) in $Sr_3Ru_2O_7$ is a prerequisite for understanding these physical properties, especially, for correlating changes in crystal structure to magnetic and transport phenomena observed at low temperatures.

$Sr_3Ru_2O_7$ is a member of a family of materials with the $Sr_3Ti_2O_7$-type structure (7) and with the chemical formula $A_3M_2O_7$ (A = alkaline/rare earth metal, M = transition metal), where M occupies the center of an octahedron of oxygen atoms and A is located in the cages formed between these octahedra (Fig. 1). When A is large, the network of octahedra is under tension and the corner-sharing MO_6 octahedra can form a high symmetry structure with no distortion. When M is large, the network of octahedra is under compression, leading to buckling at the shared oxygen apexes, which is accommodated by cooperative

[1] Permanent address: Department of Physics, Ben-Gurion University of the Negev, P. O. Box 653, Beer Sheva 84190, Israel.

[2] Permanent address: Physical Science Division, Electrotechnical Laboratory, Umezono 1-1-4, Tsukuba 305-8568, Japan.

0022-4596/00 $35.00

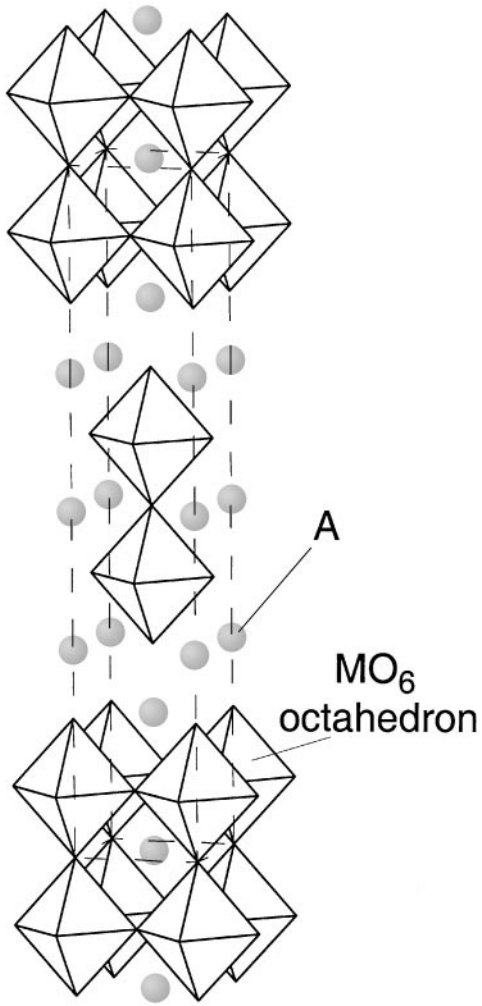

FIG. 1. The crystal structure of $A_3M_2O_7$ with the $Sr_3Ti_2O_7$-type structure. It consists of bilayers of M-centered oxygen octahedra and belongs, if undistorted, to the $I4/mmm$ space group. The A ions (shaded spheres) and the a_0 by c_0 unit cell (dashed line) are shown.

rotations of the octahedra. The transition between these two states will occur at a "zero strain" point where the ionic sizes of M and A exactly match the sizes of their respective cages. This can be formulated into a geometrical requirement, namely $(R_A + R_O)/(R_M + R_O) = \sqrt{2}$, where R_M, R_A, and R_O are ionic radii for M, A, and O. Using $R_O = 1.40$ Å (8), the relation $R_M = 0.71\ R_A - 0.41$ is obtained for the "zero strain line" in R_M vs R_A space. Above this line, the octahedral network is under compression and distortions are expected. Of the nine previously studied $A_3M_2O_7$ compounds, six with no distortions appear below this line, whereas three with distortions appear above the line (Fig. 2). The structure of the compounds with no distortions or disordered distortions belongs to the tetragonal $I4/mmm$ space group (9), with $a_0 \sim 3.9$ Å, $c_0 \sim 20$ Å (Fig. 1), and $Z = 2$.

In the present paper we report the results of a study of the crystal structure of $Sr_3Ru_2O_7$ at room temperature in polycrystals, with special attention to structural distortions. Since the ionic radii of Sr^{2+} and Ru^{4+} (1.44 and 0.62 Å (8)) place this material above the zero strain line, we expect, and indeed find, this material to be distorted. The structural distortions correspond to a pure rotational mode and are highly ordered. This result is in agreement with an earlier electron diffraction result (18), and in contrast to a recent neutron powder diffraction result where semi-ordered distortions are proposed (19) for this material.

EXPERIMENT

A polycrystalline sample of $Sr_3Ru_2O_7$ was prepared by a conventional method of solid state reaction as follows. A stoichiometric mixture of powders of $SrCO_3$ (99.99%) and RuO_2 (99.9%) was ground and pressed into pellets. The pellets were sintered in air at 1173, 1423, and 1573 K each for 24 h. The sample was then left to cool in the furnace and was taken out of the furnace after 2 h when it reached 673 K. This is in contrast to other preparation methods where the sample was quenched from the highest temperature (19). X-ray diffraction (XRD) did not reveal any impurity lines. However, the amount of ferromagnetic impurity $SrRuO_3$ ($T_C = 160$ K) was estimated at about 1% from the temperature dependence of the magnetic susceptibility. As was observed in previous preparations (5),

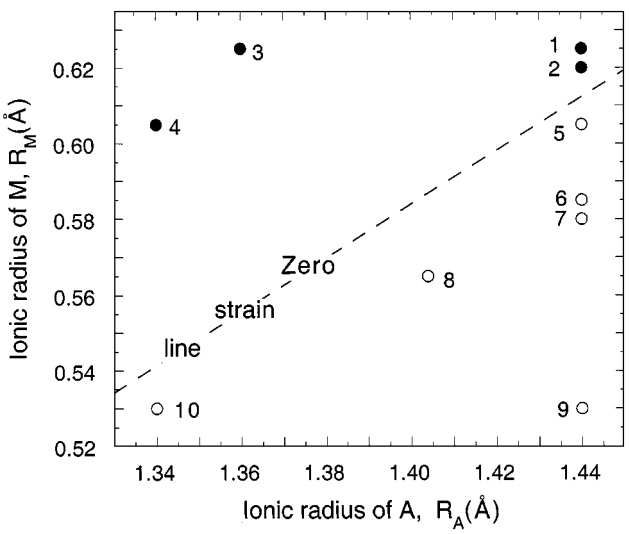

FIG. 2. A diagram of R_M vs R_A for $A_3M_2O_7$ materials with the $Sr_3Ti_2O_7$-type structure (R_M = ionic radius (8) of M). (1) $Sr_3Ir_2O_7$ (10), (2) $Sr_3Ru_2O_7$ (present work), (3) $La_3Ni_2O_7$ (11), (4) $Ca_3Ti_2O_7$ (12), (5) $Sr_3Ti_2O_7$ (12), (6) $Sr_3Fe_2O_7$ (13), (7). $Sr_3V_2O_7$ (14), (8) $La_{1.4}Sr_{1.6}Mn_2O_7$ (15), (9) $Sr_3Mn_2O_7$ (16), and (10) $Ca_3Mn_2O_7$ (17). Materials with (solid circles) and without (open circles) distortion are shown, together with the calculated zero strain (dashed) line. Note that distorted/undistorted materials appear above/below this line as predicted.

magnetic susceptibility vs temperature showed a maximum at about 20 K, and the electrical resistivity vs temperature showed a metallic behavior.

The neutron diffraction data were collected at room temperature for a 5.32-g sample by the time-of-flight technique using the Special Environment Powder Diffractometer (SEPD) (20) at the Intense Pulsed Neutron Source (IPNS). Superlattice reflections (SLR) were observed (Fig. 3) in the phase pure diffraction pattern, which was therefore indexed with respect to a $\sqrt{2}a_0 \cdot \sqrt{2}a_0 \cdot c_0$ supercell. This supercell (Fig. 4) corresponds to a unit cell in the (nonstandard) space group $F4/mmm$ of the undistorted lattice and is twice the volume of the standard $I4/mmm$ unit cell (Fig. 1) (7, 9). The following SLRs were observed: 212, 123, 214, 218, 129, 321, 232, 12$\underline{1}$3, 141, 412, 238, and 143. These SLRs satisfy the condition that $h + l = 2n$ and, hence, require a lattice with a centered face perpendicular to the b axis (i.e., a B lattice (9)). The first three SLRs were also observed in a high-statistics XRD measurement with the same relative intensities as in the neutron diffraction.

SURVEY OF POSSIBLE DISTORTED STRUCTURES

It is well known that perovskite and perovskite-related structures distort predominantly through rotations of rigid oxygen octahedra (21). Exceptions to this rule are found with very large distortions when there is an appreciable distortion of the unit cell. In the present case, it is found that the unit cell is not distorted ($a = b$); hence, only distortions resulting from rotations of the oxygen octahedra are expected. The number of allowed rotations is significantly reduced due to the constraint imposed by the shared apexes of neighboring octahedra. There are only eight modes of pure rotations (i.e., rotations about symmetry axes) possible (Fig. 5), consistent with the observed unit cell (Fig. 4). Each one is related to a different phonon mode. These modes belong to space groups (Table 1) that are subgroups of order 4 or 8 of the space group, $I4/mmm$ of the undistorted structure (Fig. 6) (9).

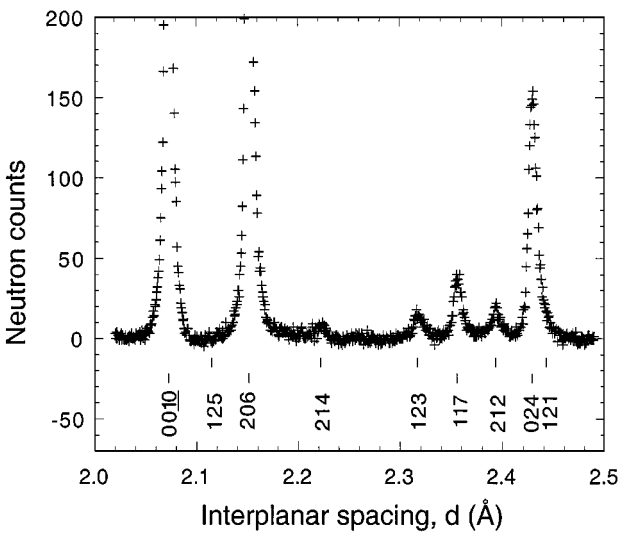

FIG. 3. A portion of the observed neutron diffraction profile of $Sr_3Ru_2O_7$. The reflections are indexed with respect to the unit cell delineated in Fig. 4. Three observed reflections, though consistent with the unit cell, do not belong to the F lattice. They (upper tick marks) belong to a superlattice, which is obtained by removing two face-centered translations, $\frac{1}{2}, \frac{1}{2}, 0$ and $0, \frac{1}{2}, \frac{1}{2}$ from the F lattice.

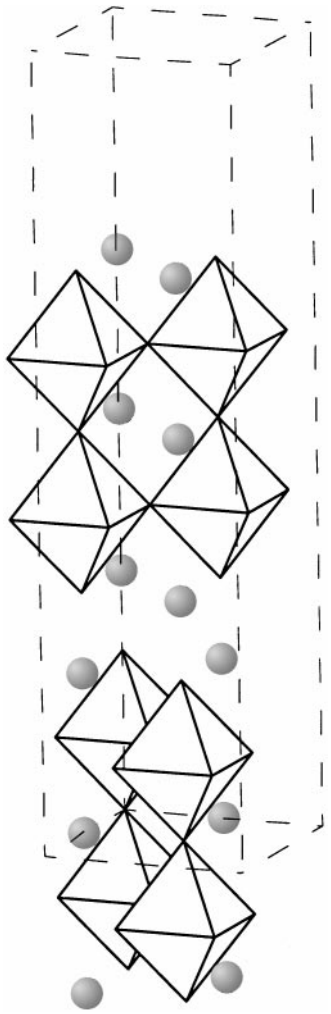

FIG. 4. The supercell used in the present work. The corresponding lattice parameters are $a = \sqrt{2}a_0$ and $c = c_0$, rendering a volume which is twice the volume of the undistorted $I4/mmm$ unit cell (Fig. 1). In this unit cell the bioctahedrons are placed at 0, 0, 0; $\frac{1}{2}, \frac{1}{2}, 0$; $\frac{1}{2}, 0, \frac{1}{2}$; and $0, \frac{1}{2}, \frac{1}{2}$; underscoring the $F4$ (nonstandard) tetragonal lattice of the undistorted structure.

STRUCTURE DETERMINATION

Selection rules. From the selection rules on allowed SLRs (see Experiment) it is concluded that the structure

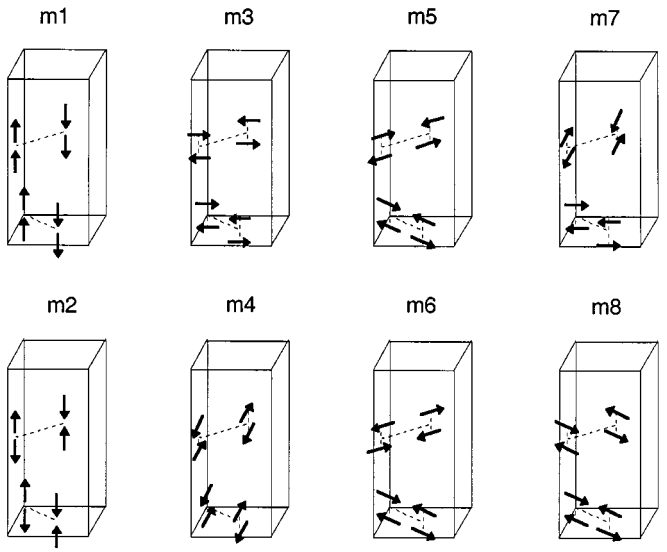

FIG. 5. The possible distorted structures of $Sr_3Ru_2O_7$, derived from simple rotations (i.e., rotations about symmetry axes) of rigid octahedra, consistent with the unit cell of Fig. 4. Each octahedron of Fig. 4 is replaced by an arrow which represents the sense of rotation of the octahedron. The space groups to which these structures belong are listed in Table 1.

must have a *B* lattice. This result rules out structures with tetragonal symmetry (i.e., m5, m6, and m7 (Fig. 5)).

Comparison of neutron and X-ray diffraction. The relative intensities of the SLRs 212, 123, and 214 observed in XRD are equal to those observed in the neutron diffraction. This implies that the contribution to these reflections comes from a single atomic species that distorts and lowers the *I*4/*mmm* (*F*4/*mmm*) symmetry of the undistorted structure. This observation suggests that oxygen atoms alone contribute to the observed distortion and is consistent with limiting the search to structural models with rotation of the oxygen octahedra.

Preliminary Rietveld analysis. The powder diffraction data were analyzed using the Rietveld program GSAS (22) for several structural models (Table 1). The undistorted (*I*4/*mmm*) structure (I1 in Table 1) yielded a poor fit with anomalously large U_{11} for the oxygen atoms in the Ru plane. Upon introducing disordered rotations of the octahedra about the *c* axis, which can be modeled by using split oxygen atom positions in the *I*4/*mmm* space group, a reasonable value of U_{11} and a considerable improvement in the fit were obtained. These results alone indicate displacements of oxygen atoms in the *xy* plane and, hence, point to m1 and m2 (Fig. 5) as the most probable structures.

Rietveld analysis. Next, each one of the eight structural models (Fig. 5) was fully refined. The structure m2, orthorhombic space group *Bbcb*, yielded by far the best fit of the eight structures (Table 1). The structures m5, m6, and m7, which do not satisfy the selection rules on the allowed SLRs, gave a very poor fit to the observed data. The combination of rotations m1 + m3 (found in $Ca_3Ti_2O_7$ (12)) yielded a poor fit, whereas m2 + m4 did not yield an improved fit compared to m2.

Stability of the solution. In order to test the stability of this (m2) solution against interbilayer disorder, we "unconstrained" the interbilayer order in the rotations of the oxygen atoms in the Ru planes (O3 in Table 2) by adding oxygen atoms that rotate in the opposite sense (O4 in Table 2). When refined under the constraint that the sum of

TABLE 1
Structural Models of $Sr_3Ru_2O_7$ with Distortions Consisting of Rotations of the Oxygen Octahedra, Their Space Groups, Symmetry Reduction with Respect to the Undistorted Structure, and a Summary of the Results of the Rietveld Analysis

Mode	Space group	Sym. reduc.	Angle (°)	χ^2	R_{wp} (%)	R_p (%)
I1	D_{4h}^{17} - *I*4/*mmm*, #139	1	0	6.153	10.78	8.01
I2	D_{4h}^{17} - *I*4/*mmm*, #139	1	6.8 (1)	4.032	8.72	6.05
m1	D_{2h}^{18} - *Bbcm*, #64	4	5.4 (1)	4.744	9.46	6.53
m2	D_{2h}^{22} - *Bbcb*, #68	4	6.8 (1)	2.384	6.71	4.62
m3	D_{2h}^{17} - *Bbmm*, #63	4	3.3 (1)	5.299	10.00	7.20
m4	D_{2h}^{21} - *Bmcm*, #67	4	3.6 (1)	5.326	10.03	7.38
m5	D_{4h}^{14} - $P4_2/mnm$, #136	4	3.1 (1)	5.573	10.26	7.51
m6	D_{4h}^{10} - $P4_2/mcm$, #132	4	2.6 (2)	5.320	10.02	7.37
m7	C_{4h}^{2} - $P4_2/m$, #84	8	3.9 (1)	5.253	9.96	7.38
m8	C_{2h}^{3} - *B*112/*m*, #12	8	4.3 (1)	4.809	9.53	6.96
m1 + m3	C_{2v}^{12} - $Bb2_1m$, #36	8	5.3 + 3.0 (1)	4.363	9.07	6.31
m2 + m4	C_{2h}^{6} - *B*112/*n*, #15	8	6.6 + 0.6 (1)	2.425	6.77	4.67

Note. I1 and I2 designate the nondistorted and distorted disordered structure (no superlattice reflections). mi's ($i = 1,..,8$) are defined in Fig. 5. The structure proposed by the present study is m2.

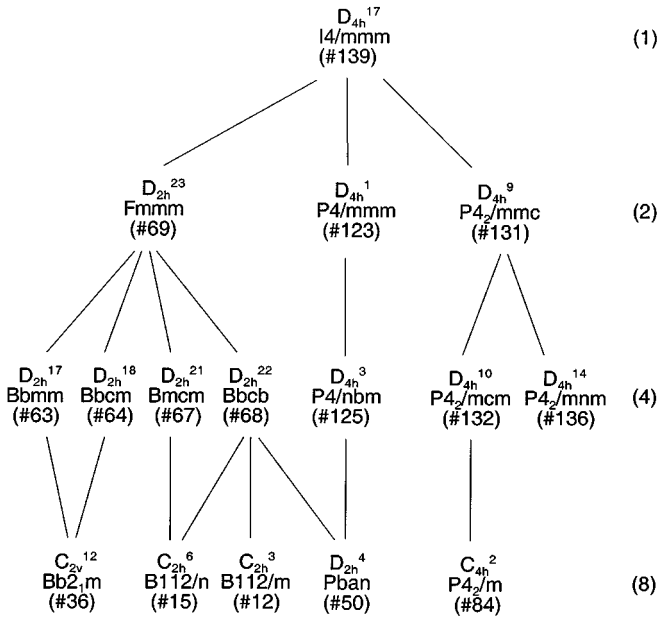

FIG. 6. Group–subgroup relations for the eight simple structures of Fig. 5, and for other structures which are derived from the $Sr_3Ti_2O_7$ type, previously reported for other materials. The order of the subgroup (symmetry decrease) is listed on the right (in parenthesis).

the fractions (site occupancies) of the two atoms is equal to 1, this refinement converged to essentially the ordered solution (m2) with a small fraction ($\sim 4\%$) of disorder (see below), showing that the choice of interbilayer order is justified.

Conclusion of the crystal structure determination. It is concluded that m2, which we shall call the *ordered model*, is the crystal structure consistent with our data. The Rietveld profile calculated for the ordered model, with the observed data, is shown in Fig. 7. The refined parameters for this structure with other information are summarized in Table 2.

It is a valid question to ask whether any of the subgroups of *Bbcb* provide a better fit to the data. We see no evidence in our raw data for any additional reflections that would suggest a lower symmetry. Also, the temperature factors do not suggest additional static displacements, and the identical refined values for the orthorhombic lattice parameters a and b suggest that the distortion involves only pure rotations. We have not made an exhaustive investigation of all possible lower symmetry models, but all lower symmetry models we investigated converged to the face-centered *Bbcb* solution. If additional atom displacements or disorder exists, it will likely require single-crystal data to see them.

DESCRIPTION OF THE ORDERED MODEL

The undistorted crystal structure is shown in Fig. 1. Consider one bilayer of RuO_6 octahedra, where every octahedron is rotated about the c axis, and in each bioctahedron the sense of rotation is reversed across the shared apical

TABLE 2
Structural Parameters and Refinement Information for $Sr_3Ru_2O_7$

Atom	x	y	z	Fraction	U_{iso} (Å^2/100)	$U_{11} = U_{22}$ (Å^2/100)	U_{33} (Å^2/100)	U_{12} (Å^2/100)
Ru	$\frac{1}{4}$	$\frac{1}{4}$	0.40298 (7)	1.0	—	0.20 (3)	0.48 (5)	0.24 (8)
Sr1	$\frac{1}{4}$	$\frac{1}{4}$	0	1.0	0.68 (4)	—	—	—
Sr2	$\frac{1}{4}$	$\frac{1}{4}$	0.18631 (6)	1.0	0.80 (4)	—	—	—
O1	$\frac{1}{4}$	$\frac{1}{4}$	$\frac{1}{2}$	1.0	—	1.55 (9)	0.5 (1)	—
O2	$\frac{1}{4}$	$\frac{1}{4}$	0.30448 (8)	1.0	—	0.95 (6)	1.4 (1)	0.3 (1)
O3	0.5293 (2)	− 0.0293 (2)	0.09710 (8)	0.959 (5)	0.80 (3)	—	—	—
O4	0.4707 (2)	0.0293 (2)	0.09710 (8)	0.041 (5)	0.80 (3)	—	—	—

Lattice parameters (Å): $a = 5.5006$ (4) $b = 5.5006$ (4) $c = 20.725$ (1)

Space group: *Bbcb* (#68)
Coordinates: $(0, 0, 0) + (1/2, 0, 1/2) +$
$\mp (x, y, z \quad -x, 1/2 + y, z \quad x, -y, 1/2 + z \quad -x, 1/2 - y, 1/2 + z)$
Constraints: $x(O3) + x(O4) = 1$, $y(O3) + y(O4) = 0$, $x(O3) + y(O3) = 1/2$, $z(O3) = z(O4)$,
$U_{iso}(O3) = U_{iso}(O4)$, Fraction (O3) + Fraction (O4) = 1, $U_{11} = U_{22}$

Range of d spacing (Å): 0.5 to 3.95
No. of data points: 5152 No. of reflections: 1372 No. of variables: 38
$\chi^2 = 2.384$ R_{wp} (%) = 6.71 R_p (%) = 4.62

Bond lengths (Å): Ru–O1 = 2.012 (2) Ru–O2 = 2.039 (2) Ru–O3 = 1.9582 (2)

Note. The numbers in parentheses are equal to the standard deviations and represent the statistical error of the last significant digit. Parameters without errors were fixed throughout the refinement.

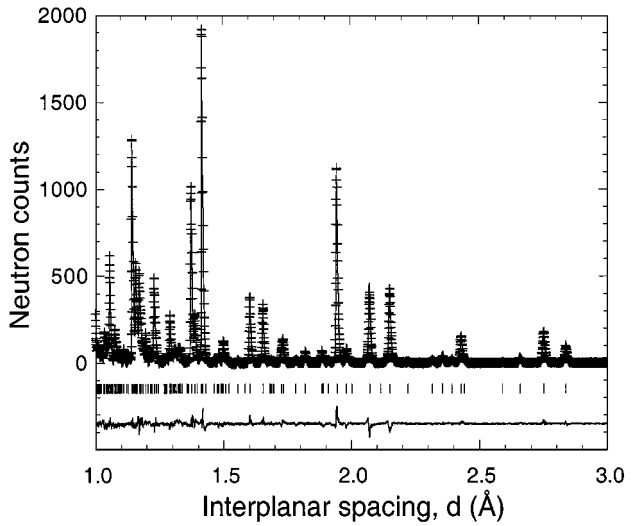

FIG. 7. The neutron diffraction data collected for the $Sr_3Ru_2O_7$ sample (+) with the calculated Rietveld refinement profile (solid line) of the ordered model. The orthorhombic space group *Bbcb* (#68) was used in the calculations. The background was fitted as part of the refinement, but has been subtracted before plotted. Tick marks below the diffraction profile, mark the calculated positions of the allowed reflections. A difference curve (observed minus calculated) is drawn at the bottom.

oxygen atom. This is represented in Fig. 5 by outward (or inward) pairs of arrows. Given a bioctahedron with a certain sense of rotation (say outward arrows), its four close neighbor bioctahedrons are constrained (by the shared oxygen atoms) to have an opposite sense of rotation (i.e., inward arrows). There is no frustration in this mode of ordering; hence, a long range order of the bioctahedrons with two senses of rotations (i.e., inward and outward) is established in two dimensions (2D). This bilayer with 2D ordered rotations is the building block of the ordered model, obtained by repeatedly using *B* translations (i.e., 1/2 0 1/2) to stack these bilayers along the *c* axis. This interbilayer ordering establishes a long-range order along the *c* axis, in addition to the 2D intrabilayer long-range ordering, yielding altogether a structure where the rotations have 3D long-range order. Our analysis shows that $\sim 4\%$ of the bilayers consist of bioctahedrons with an opposite sense of rotation (Table 1, see fraction of O4). These are stacking errors (sometimes called stacking faults) in the *B* stacking, and represent interbilayer disorder. A stacking error occurs at random along *c* when, in a *B* stacking, a bilayer is obtained from its close neighbors through an *A* (i.e., 0 1/2 1/2) rather than a *B* translation. Stacking faults amounting to a few percent, depending on preparation, are not uncommon in layered materials.

COMPARISON WITH THE SEMI-ORDERED MODEL

In a previous paper Huang *et al.* (19) reported a structure (deduced from neutron powder diffraction) of $Sr_3Ru_2O_7$, different from our structure (i.e., the ordered model) reported here. Their structure consists of different stacking of the same building blocks used in the ordered model. It is obtained by stacking half of the bilayers along *c*, with interbilayer order, by repeatedly using the *c* translation (i.e., 0 0 1). The other half, interleaved between the bilayers of the first half, are stacked with intrabilayer disorder, using, at random, the *A* and *B* translations. This structure, therefore, represents a *semi-ordered model* and belongs to a *P* lattice.

Huang *et al.* refined this structure in the space group *Pban*. However, they imposed constraints that define a higher symmetry and imposed interbilayer disorder in half of the bilayers. Specifically, Huang *et al.* imposed two kinds of constraints. First, they constrained atom positions (e.g., $y = 1/2 - x$, see their Table 2) and the lattice parameters ($a = b$) in such a way that the orthorhombic *Pban* symmetry is transformed to that of the tetragonal space group *P*4/*nbm*. Thus, we have performed the refinements in the constrained *Pban* model of Huang *et al.* and in *P*4/*nbm* and obtained identical results. In this paper, in order to not confuse readers who are not conversant with the crystallography, we compare our refinement in *Bbcb* with a refinement done in *Pban* with the same constraints used by Huang *et al.* (Table 3). Our refinement of the ordered model in *Bbcb* gives a substantially better fit than a refinement using the semi-ordered of Huang *et al.* in *Pban*.

The second constraint of Huang *et al.* involves the site occupancies of the four oxygen atom positions in the planes of the Ru atoms (8m sites in their Table 2). These four site occupancies are constrained to the values 1.0, 0.0, 0.5, and 0.5, which define a rather complex pattern of order and disorder. The rotations of the RuO_6 octahedra in alternate bilayers have a full interbilayer order (site occupancies 1.0 and 0.0), while the rotations in the intervening bilayers (site occupancies 0.5 and 0.5) have a full interbilayer disorder. Using the *Pban* model of Huang *et al.*, we removed these constraints on site occupancies and let the site occupancies refine, while

TABLE 3

Fit Criteria (23) for the Refinements of the Ordered Model of the Present Study in the *Bbcb* Representation, and for the Previously Published (19) Semi-ordered Model in the *Pban* Representation

Fit criterion	*Bbcb* ordered	*Pban* semi-ordered	
		u	*v*
χ^2	2.410	2.764	2.634
R_{wp} (%)	6.74	7.23	7.05
R_p (%)	4.66	5.10	4.94

Note. The refinements were performed using isotropic thermal parameters (as was done in Ref. 19). When the constraints on site occupancies in *Pban* (column 4) are removed (see text), it converges to the ordered model (column 2).

u = Crystal parameters (except lattice parameters) as published (19). v = Refined crystal parameters.

retaining the constraints on atom positions (which define pure rotations of the RuO_6 octahedra around the *c* axis and keep the bilayers equally spaced). This refinement converged smoothly to a solution identical to the one we achieved using the face-centered space group *Bbcb* which is a supergroup of *Pban* (Fig. 6), with a substantial improvement in the fit.

These refinement tests show that the ordered model we report and not the semi-ordered model is consistent with our neutron data. It is possible that, as a result of quenching the sample during preparation, the sample studied by Huang *et al.* (19) could have a different degree of disorder in the rotations of the RuO_6 octahedra than our sample. However, such a situation would likely lead to a partially ordered *Bbcb* structure (i.e., with general disorder in the sense of rotation) rather than alternating layers of RuO_6 octahedra that are either fully ordered or fully disordered, as reported by Huang *et al.*

DISCUSSION AND CONCLUSIONS

The structure of $Sr_3Ru_2O_7$ exhibits ordered rotations of 6.8° about the *c* axis, belonging to a pure mode (m2 in Fig. 5), Although it belongs to the orthorhombic space group *Bbcb* (#68) (9), our analysis shows that the lattice parameter *a* is equal to *b* within the experimental uncertainty. Distortions were reported for three other isostructural (when undistorted) materials (Fig. 2). In $Sr_3Ir_2O_7$, rotations of 12° about the *c* axis were found (10). However, the sense of rotation was reported to exhibit a complete interbilayer disorder. In $Ca_3Ti_2O_7$, large distortions (i.e., $a \neq b$) were found that consist of a mixed mode (m1 + m3) (12). In $La_3Ni_2O_7$, large distortions (i.e., $a \neq b$) were found that include distortion of the octahedra (11). These three materials together with $Sr_3Ru_2O_7$ appear above the zero strain line in Fig. 2. Six other materials, where no distortion was found, appear below the zero strain line. This suggests that the rotational distortions are of steric rather than electronic origin. The mechanism responsible for the rotation's interbilayer order or disorder is unclear at the present time. The fact that $Sr_3Ru_2O_7$ (with interbilayer order) and $Sr_3Ir_2O_7$ (with interbilayer disorder) have almost identical coordinates in R_M vs R_A space leads us to believe that it is not of steric origin.

The crystal structure determination of the present work shows that the rotations of the oxygen octahedra are ordered in 3D. This is in contrast to results reported by Huang *et al.* (19) where the rotations of only half of the octahedra are ordered in 3D. A knowledge of the correct crystal structure is needed for calculation of the electronic band structure, assignment of vibrational modes (e.g., in Raman or neutron inelastic scattering), interpretation of magnetic interactions on a microscopic scale, understanding possible structural phase transitions manifest in transport and magnetic measurements, assessing the effect of disorder on transport, and understanding the effect of extended defects such as stacking faults and their effects on physical properties.

Note added in proof: After the paper was submitted, we realized that according to Landau Theory and renormalization group theory (24), the transition to *Bbcb* (present work) is allowed to be continuous, whereas a transition to *Pban* (as proposed by Huang *et al.* (19) is not allowed to be continuous.

ACKNOWLEDGMENTS

The authors thank S. Short for her technical support and for her assistance with the powder neutron diffraction measurements. This work was supported by the National Science Foundation, Office of Science and Technology Centers, under Grant DMR 91-20000 (H.S. and O.C.) and U.S. Department of Energy, Office of Science, under Contract W-31-109-ENG-38 (J.D.J. and the operation of IPNS), by Ben-Gurion University of the Negav (H.S.), and by the ARPA/ONR at NIU (O.C.).

REFERENCES

1. J. G. Bednorz and K. A. Muller, *Z. Phys. B* **64,** 189 (1986).
2. Y. Maeno, H. Hashimoto, K. Yoshida, S. Nishizaki, T. Fujita, J. G. Bednorz, and F. Lichtenberg, *Nature* **372,** 532 (1994).
3. Y. Moritomo, A. Asamitsu, H. Kuwahara, and Y. Tokura, *Nature* **380,** 141 (1996).
4. R. J. Cava, H. W. Zandbergen, J. J. Krajewski, W. F. Peck, Jr., B. Batlogg, S. Carter, R. M. Fleming, O. Zhou, and L. W. Rupp, Jr., *J. Solid State Chem.* **116,** 141 (1995).
5. S. Ikeda, Y. Maeno, and T. Fujita, *Phys. Rev. B* **57,** 978 (1998); S. Ikeda and Y. Maeno, *Physica B* **259–261,** 947 (1999); S. Ikeda, Y. Maeno, M. Kosaka, and Y. Uwatoko, *Phys. Rev. B* **62,** 1 (2000).
6. G. Cao, S. McCall, and J. E. Crow, *Phys. Rev. B* **55,** 672 (1997).
7. S. N. Ruddlesden and P. Popper, *Acta Crystallogr.* **11,** 54 (1958).
8. R. D. Shannon, *Acta Crystallogr. Sect. A* **32,** 751 (1976).
9. T. Hahn (Ed.), "International Tables for Crystallography," Vol. A. Reidel, Dordrecht, 1983.
10. M. A. Subramanian, M. K. Crawford, and R. L. Harlow, *Mater Res. Bull.* **29,** 645 (1994).
11. Z. Zhang, M. Greenblatt, and J. B. Goodenough, *J. Solid State Chem.* **108,** 402 (1994).
12. M. M. Elcombe, E. H. Kisi, K. D. Hawkins, T. J. White, P. Goodman, and S. Matheson, *Acta Crystallogr. Sect. B* **47,** 305 (1991).
13. S. E. Dann, M. T. Weller, and D. B. Currie, *J. Solid State Chem.* **97,** 179 (1992).
14. N. Suzuki, T. Noritake, N. Yamamoto, and T. Hioki, *Mater. Res. Bull.* **26,** 1 (1991).
15. D. N. Argyriou, J. F. Mitchell, P. G. Radaelli, H. N. Bordallo, D. E. Cox, M. Medarde, and J. D. Jorgensen, *Phys. Rev. B* **59,** 8695 (1999).
16. J. F. Mitchell, J. E. Millburn, M. Medarde, J. D. Jorgensen, and M. T. Fernandez-Diaz, *J. Solid State Chem.* **141,** 599 (1998).
17. K. Tenida and T. Kitamura, *Tohoku Daigaku Senko Seiren Kenkyusho Iho* **37,** 33 (1981).
18. Y. Inoue, M. Hara, Y. Koyama, S. Ikeda, Y. Maeno, and T. Fujita, *in* "Advances in Superconductivity IX" (S. Nakajima and M. Murakami, Eds.). Springer-Verlag, Berlin, 1997.
19. Q. Huang, J. W. Lynn, R. W. Erwin, J. Jarupatrakorn, and R.J. Cava, *Phys. Rev. B* **58,** 8518 (1998).
20. J. D. Jorgensen, J. Faber, Jr., J. M. Carpenter, R. K. Crawford, J. F. Haumann, R. L. Hittermann, R. Kleb, G. E. Ostrowski, F. J. Rotella, and T. G. Worlton, *J. Appl. Crystallogr.* **22,** 321 (1989).
21. A. M. Glazer, *Acta Crystallogr. Sect. B* **28,** 3384 (1972).
22. A. C. Larson and R. B. Von Dreele, LAUR 86-748 (1985).
23. R. A. Young, "The Rietveld Method," p. 21. Oxford Univ. Press, Oxford, 1993.